h-BN → w-BN phase transition under dynamic–static compression

S. S. BATSANOV, S. M. GAVRILKIN, L. I. KOPANEVA, I. I. MAKSIMOV
Center for High Dynamic Pressure, Mendeleevo 141 570, Russia

M. A. MEYERS, H. C. CHEN
Department of Applied Mechanics and Engineering Science, University of California, San Diego, La Jolla, CA 92093-0411, USA

R. PRÜMMER
Ernst Mach Institute, Freiburg D-7800, Germany

E. E. SEIKO, V. A. VAZYULIN
Center for High Dynamic Pressure, Mendeleevo 141 570, Russia

Shock compression has been known to induce phase transitions in solids since 1956 [1]. The synthesis of dense forms of BN is an application of this concept: it presents considerable technological potential. Many investigations have been made on BN polymorphic transition under static and dynamic compression [2–6]. In 1967, Adadurov *et al.* [5] obtained hexagonal BN (h-BN) transformed to wurtzite BN (w-BN) under shock compression (~20 GPa). Akashi *et al.* [6] performed shock compression in the range 60–200 GPa on w-BN and zinc blende (z-BN) and found w-BN → z-BN phase transition around 100 GPa. w-BN → graphite-like BN (g-BN) and z-BN → g-BN above 100 GPa. The objective of this letter is to report results of the application of the dynamic–static compression (DSC) method developed by Batsanov [7] to the phase transition of h-BN: the microhardness, X-ray analysis and microstructure are also discussed.

The experimental set-up used is shown in Fig. 1a. The capsule, filled with KBr, ensures static pressure after the dynamic (shock) compression. For dynamic loading an explosive with a detonation velocity of 7.85 km s^{-1} was used, while the static pressure was maintained by the B2 → B1 phase transition in KBr (an active component of the working body) during unloading. This is shown in Fig. 1b. The evolution of shock-wave velocity u_s along the axis of the capsule (~3 mm) measured by ultrafast photo-registrator, is shown in Fig. 2. The dynamic pressure in the working body during shock-wave propagation from the top to the bottom of the capsule changed from 4 to 247 GPa. The distribution of dynamic pressure on the top of the capsule with h-BN was measured by manganese gauges. It was 247 GPa at the centre, and decreased to 19 GPa at the periphery.

After shocking the capsule and extracting the specimen, the sample was studied by various physico-chemical methods. The density of the specimen was measured by picnometry, yielding 3.25 g cm^{-3}. Vickers microhardness measured on the top and the bottom surfaces were slightly
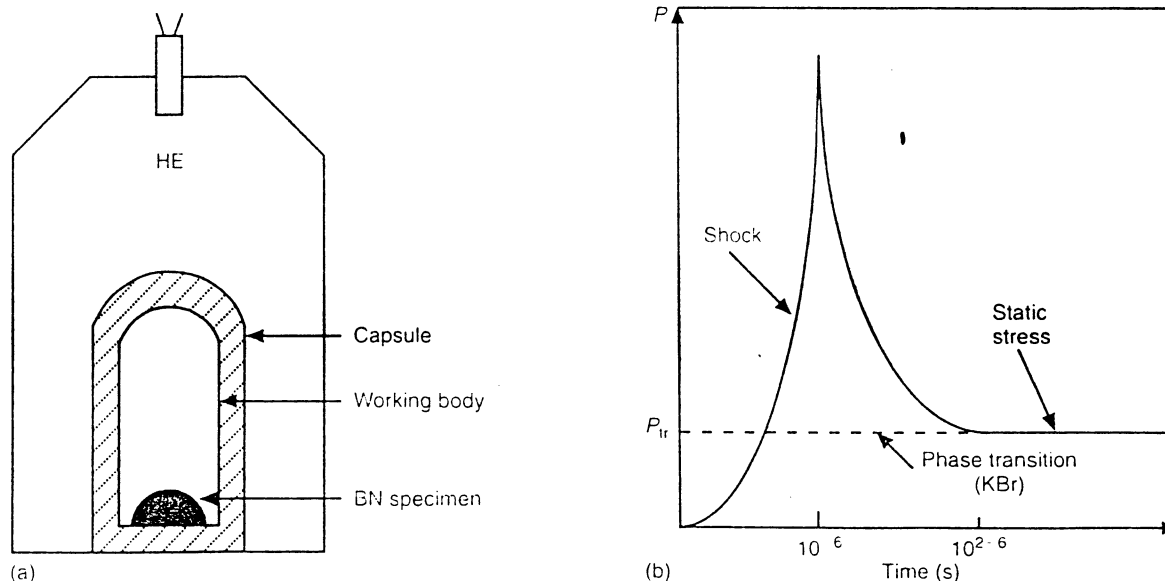
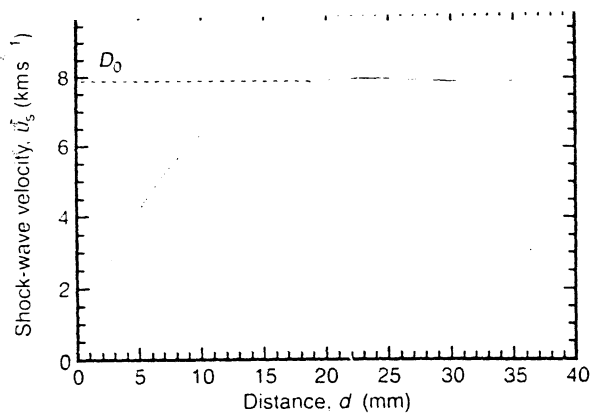Figure 2 Evolution of shock-wave velocity u_s along the cylindrical axis from the top ($d = 0$) to the bottom ($d = 35$ mm) of the capsule.

different: average 5100 for the top and 4400 at the bottom. The difference in the microhardness between top and bottom surfaces is due to the different pressure during shock compression. Fig. 3 shows the hardness distribution on the top surface. The maximum hardness in the centre of the disk corresponds to the maximum pressure along the capsule axis, therefore the minimum on the curve should reveal a nonlinear slump of pressure from the centre to the periphery. It is noteworthy that similar periodic alternations of hardness along the cross-section of a cylindrical ampoule have been observed by Japanese researchers in compressed graphite [8].

The propagation velocity of longitudinal waves was measured by the ultrasonic method (of the frequency 7–10 MHz), using a buffer rod, and was found to be equal to 9.3 km s^{-1}. The w-BN produced by the DSC method exhibited longitudinal wave speed of 8.9 km s^{-1}. The electrical conductivity measurements proved the specimen to be an insulator, and the value was equal to $\sim 5 \times 10^{14}$ Ω s^{-1}. Dielectric constant of 7.5 was measured by the condenser technique, as compared to 4.0 for the original h-BN, and the standard value of 7.1 for c-BN [9].

The prepared w-BN was chemically inert: even a 72 h treatment by concentrated HCl, HNO$_3$ and H$_2$SO$_4$ did not affect the mass of the specimen, and
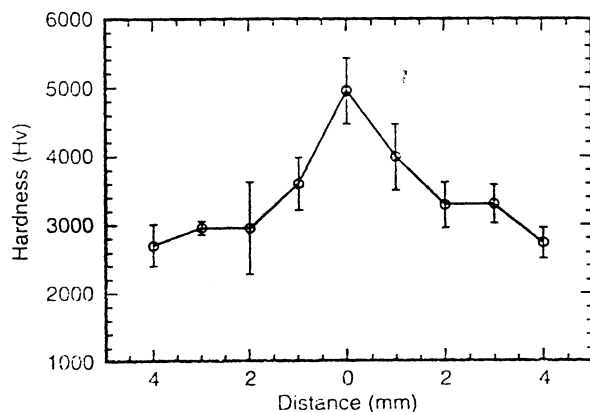
an equivalent treatment by concentrated KOH only caused a loss of mass of about 0.1%.

An X-ray powder diffraction study (DRON-4 diffractometer, CuK_α radiation) identified the product as w-BN with an admixture of $\sim$3% of original h-BN, the concentration of which decreased with the increase of hardness. The only observed reflection of h-BN, (0 0 2), is very widened and asymmetric, with its maximum corresponding to the normal $d = 0.333$ nm, but its centre to $d = 0.325$ nm, in agreement to our early observation that shock compression reduces the interlayer distance in h-BN [10].

The diffraction pattern of w-BN obtained from solid disks, shown in Fig. 4, exhibited abnormally strong (0 0 2) reflection, 2–2.5 times stronger than (1 0 0). Grinding the disk into powder removed this effect, reducing the intensity of (0 0 2) to $\sim$80% of (1 0 0), close to theoretical exception, and also significantly weakened the (0 0 2) reflection of h-BN. Apparently, the texture of the original h-BN flakes, with their (0 0 1) planes parallel to the bases of the disk, gives rise to a similar texture of w-BN, the martensite h-BN — w-BN transition proceeding via puckering of planar graphite-like hexagonal layers. Both textures were removed by grinding.

Harmonic analysis of reflection profiles yields the area of coherent scattering in the prepared w-BN of 9–10 nm, with microstrain $\varepsilon = 3.5 \times 10^3$. The reflection widths differ more than three-fold. (1 0 0) and (0 0 2) being the narrowest and (1 0 3) the widest, indicating considerable anisotropy of defects.

Backscattered electron micrographs of fracture surfaces and polished surfaces on the top and bottom are shown in Figs 5 and 6. The fracture surface exhibited intergranular property, and the grain was pulled out along the grain boundaries (Fig. 5). This result indicates the weak interparticle bonding in w-BN. Fig. 6 shows that the grain size in w-BN is 200–400 nm, with high porosity. These fine grains

Figure 3 Distribution of Vickers microhardness on the top surface of w-BN along the cross-section of the cylinder axis.
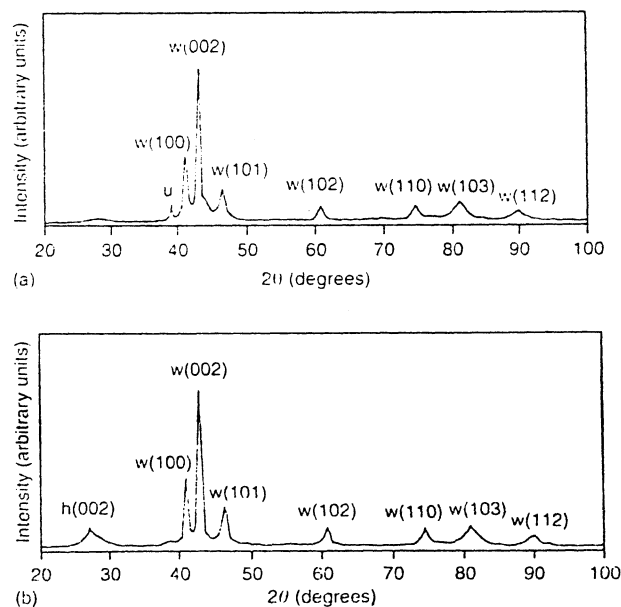

(a)

(b)

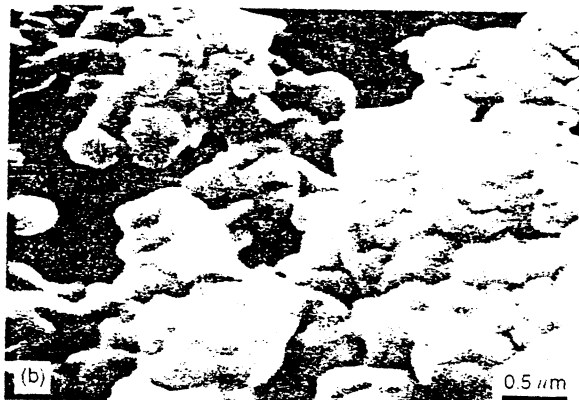Figure 4 X-ray diffraction patterns of solid w-BN disk: (a) top surface and (b) bottom surface.
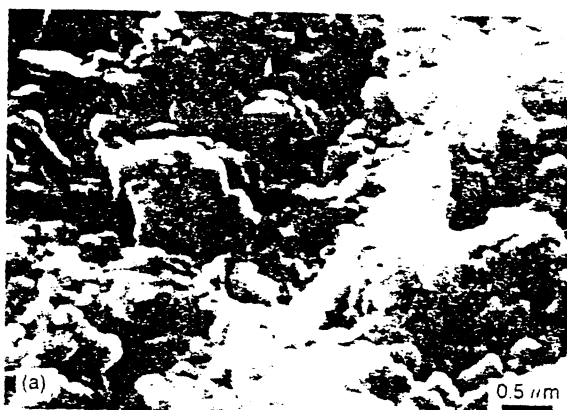
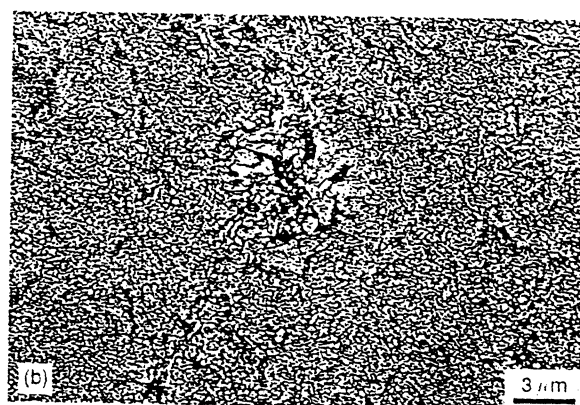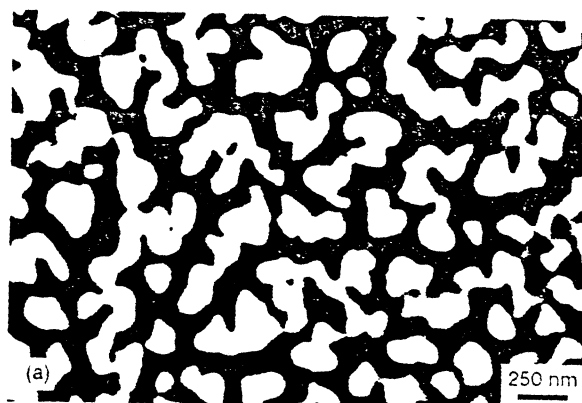Figure 5 Backscattered electron micrographs of fracture surfaces of w-BN.

Figure 6 Backscattered electron micrographs of polished w-BN: (a) top surface and (b) bottom surface.

were formed during the shock compression and performed the weakly bonded. Similar results in c-BN were observed by Akashi and Sawaoka [11].

Acknowledgements

References

1. D. BANCROFT, E. PETERSON and S. MINSHALL, J. Appl. Phys. 27 (1956) 291.
2. R. H. WENTORF, J. Chem. Phys. 26 (1957) 956.
3. F. P. BUNDY and R. H. WENTORF, ibid. 38 (1963) 1144.
4. S. S. BATSANOV, G. E. BLOKHINA and A. A. DERIBAS, J. Struct. Chem. 7 (1965) 209.
5. G. A. ADADUROV, Z. G. ALIEV, L. O. ATOVMYAN, T. V. BAVINA, YU.G. BOROD'KO, O. N. BREUSOV, A. N. DREMIN, A. KH. MURANEVICH and S. V. PERSHIN, Sov. Phys. Dokl. 12 (1967) 173.
6. T. AKASHI, H. R. PAK and A. B. SAWAOKA, J. Mater. Sci. 21 (1986) 4060.
7. S. S. BATSANOV, in Proceedings of the 2nd International Symposium on Intense Dynamic Loading and its Effects, Chengdu, China, 1992, p. 844.
8. Y. NOMURA and Y. HORIGUCHI, J. Ind. Explosive Soc. Jpn 24 (1963) 26.
9. P. GIELISSE, S. MITRA, J. PLENDL, R. GRIFFIS, L. MANSUR, R. MARSHALL and E. PASCOE, Phys. Rev. 155 (1967) 1039.
10. S. S. BATSANOV, E. M. MOROZ and V. P. KUZYU-TIN, J. Struct. Chem. 11 (1970) 147.
11. T. AKASHI and A. B. SAWAOKA, J. Mater. Sci. 22 (1987) 1127.